INL/CON-07-12102
PREPRINT

High-Temperature Co-electrolysis of Carbon Dioxide and Steam for the Production of Syngas; Equilibrium Model and Single-Cell Tests

International Topical Meeting on the Safety and Technology of Nuclear Hydrogen

J. E. O'Brien
C. M. Stoots
J. S. Herring
J. J. Hartvigsen

June 2007

The INL is a
U.S. Department of Energy
National Laboratory
operated by
Battelle Energy Alliance

High-Temperature Coelectrolysis of Carbon Dioxide and Steam for the Production of Syngas; Equilibrium Model and Single-Cell Tests

O'Brien[1], J. E., Stoots[1]. C. M., Herring[1], J. S. and Hartvigsen[2], J. J.

[1]Idaho National Laboratory
Idaho Falls, ID

[2]Ceramatec, Inc.
Salt Lake City, UT

An experimental study has been completed to assess the performance of single solid-oxide electrolysis cells operating over a temperature range of 800 to 850ºC in the coelectrolysis mode, simultaneously electrolyzing steam and carbon dioxide for the direct production of syngas. The experiments were performed over a range of inlet flow rates of steam, carbon dioxide, hydrogen and nitrogen and over a range of current densities (-0.1 to 0.25 A/cm^2) using single electrolyte-supported button electrolysis cells. Steam and carbon dioxide consumption rates associated with electrolysis were measured directly using inlet and outlet dewpoint instrumentation and a gas chromatograph, respectively. Cell operating potentials and cell current were varied using a programmable power supply. Measured values of open-cell potential and outlet gas composition are compared to predictions obtained from a chemical equilibrium coelectrolysis model. Model predictions of outlet gas composition based on an effective equilibrium temperature are shown to agree well with measurements. Area-specific resistance values were similar for steam electrolysis and coelectrolysis.

I. INTRODUCTION

A research project is under way at the Idaho National Laboratory (INL) to investigate the feasibility of producing syngas by simultaneous electrolytic reduction of steam and carbon dioxide (coelectrolysis) at high temperature using solid-oxide cells. Syngas, a mixture of hydrogen and carbon monoxide, can be used for the production of synthetic liquid fuels via Fischer-Tropsch processes. This concept, coupled with nuclear energy, provides a possible path to reduced greenhouse gas emissions and increased energy independence, without the major infrastructure shift that would be required for a purely hydrogen-based transportation system[1]. Furthermore, if the carbon dioxide feedstock is obtained from biomass, the entire concept would be climate-neutral.

The INL co-electrolysis research program is an outgrowth of the high-temperature steam electrolysis research program funded by the Department of Energy Nuclear Hydrogen Initiative (NHI). Under the NHI, the INL has been developing efficient high-temperature hydrogen production technologies based on solid oxide fuel cell (SOFC) technology and materials[2-4]. The zirconia electrolytes used for SOFCs conduct oxygen ions, so they can be used to electrolyze H_2O to H_2 and/or CO_2 to CO. When both steam and carbon dioxide are present simultaneously in the feed stream, the total amounts of hydrogen and carbon monoxide that are produced depend on the electrolysis current. The relative amount of hydrogen produced versus carbon monoxide is determined by the relative amounts of steam, hydrogen (included in the feed stream as a reducing agent) and carbon dioxide included in the feed stream and by the effect of the shift reaction:

$$CO_2 + H_2 <=> H_2O + CO \quad (1)$$

The desired molar ratio of hydrogen to carbon monoxide in the gaseous product depends on the particular liquid fuel to be produced as a final product, but a 2-to-1 ratio of H_2 to CO is typical.

The INL co-electrolysis research program includes experimental, modeling, and computational fluid dynamics (CFD) activities. This paper will provide results of single-cell co-electrolysis experiments, with comparisons to predictions obtained from a chemical equilibrium co-electrolysis model (CECM). This model was developed for prediction of final gas compositions and thermal energy requirements.

II. EXPERIMENTAL APPARATUS

A schematic of the experimental apparatus used for single-cell co-electrolysis testing is presented in Fig. 1. Primary components include gas supply cylinders, mass-flow controllers, a humidifier, on-line dewpoint and CO_2 measurement stations, temperature and pressure measurement, high temperature furnace, a solid oxide electrolysis cell, and a gas chromatograph. Nitrogen is used as an inert carrier gas. Inlet flow rates of nitrogen, hydrogen, carbon dioxide and air are established by means of precision mass-flow controllers. Hydrogen is

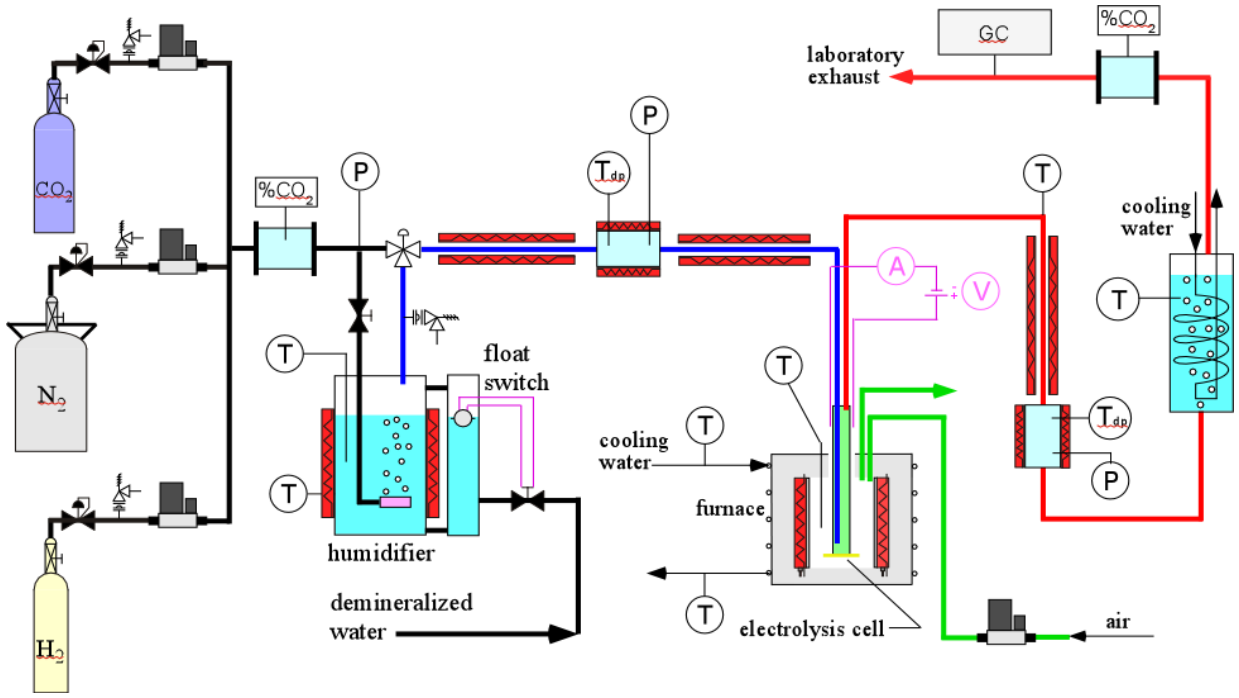

Figure 1. Schematic of single-cell co-electrolysis test apparatus.

included in the inlet flow as a reducing gas in order to prevent oxidation of the Nickel cermet electrode material. Air flow to the stack is supplied by the shop air system, after passing through a two-stage extractor / dryer unit. The nitrogen/ hydrogen / CO_2 gas mixture is mixed with steam by means of a heated humidifier. The dewpoint temperature of the nitrogen / hydrogen / CO_2 / steam gas mixture exiting the humidifier is monitored continuously using a precision dewpoint sensor. All gas lines located downstream of the humidifier are heat-traced in order to prevent steam condensation. Inlet and outlet CO_2 concentrations are also monitored continuously using on-line infra-red CO_2 sensors.

For single-cell testing, an electrolysis button cell is bonded to the bottom of a zirconia tube, as shown in Fig. 2. During testing, the tube is suspended in the furnace. This cell is an electrolyte-supported single button cell with a scandia-stabilized zirconia electrolyte, about 150 µm thick. The outside electrode, which acts as the cathode in fuel cell mode and the anode in electrolysis mode, is a doped manganite. The inside electrode (electrolysis cathode) material is a nickel cermet. Both button-cell electrodes incorporate a platinum wire mesh for current distribution. The button cell includes both an active cell area (2.5 cm^2 for the cell shown) and a reference cell area. The active cell area is wired with both power lead wires and voltage taps. The reference cell area is wired only with voltage taps, allowing for continuous monitoring of open-cell potential. The button cell is bonded to the end of a large (OD = 1.25 in., ID = 1.1 in.) zirconia tube using a glass seal. The power lead and voltage wires are routed to the far end of the zirconia tube via several small-diameter alumina tubes fixed to the outside of the zirconia manifold tube. A type-K stainless-steel sheathed thermocouple, is mounted on the manifold tube and bent around in front of the button cell in order to allow for continuous monitoring of the button-cell temperature.

The inlet gas mixture enters this tube, directing the gas to the steam/hydrogen/CO_2 side (inside) of the cell. The cell is maintained at an appropriate operating temperature (800 to 850°C) via computer-based feedback control. The furnace also preheats the inlet gas mixture and the air sweep gas. Oxygen produced by electrolysis is captured by the sweep gas stream and expelled into the laboratory. The syngas product stream exits the zirconia

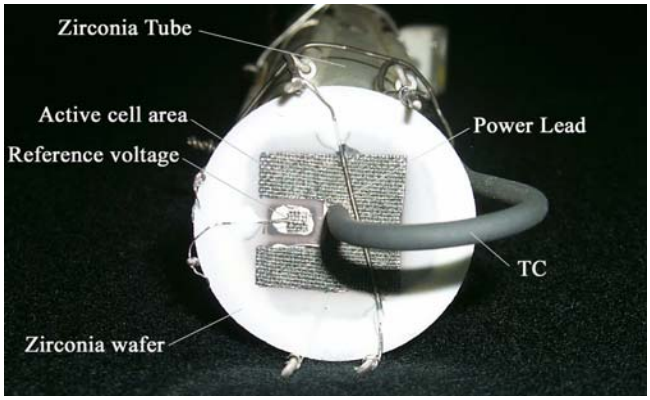

Figure 2. Detail of button cell.

tube and is directed towards the downstream dewpoint and CO_2 sensors and then to a condenser through a heat-traced line. The condenser removes most of the residual steam from the exhaust. The final exhaust stream is vented outside the laboratory through the roof. Rates of steam and CO_2 electrolysis are monitored by the measured change in inlet and outlet steam and CO_2 concentration as measured by the on-line sensors. In addition, a Gas Chromatograph (GC) has been incorporated into the facility downstream of the condenser to precisely quantify the composition of the dry constituents in the electrolysis product stream (including any CH_4 that may be produced).

III. PROCEDURE

Prior to each test, a slow automated ramp-up of the electrolysis cell temperature is performed until the desired test temperature is achieved. Heating times of 4 – 8 hours are used to take the cell from room temperature to 800ºC. During this time, the desired humidifier, humidity sensing station, and heat trace temperatures are established. Nitrogen, hydrogen, CO_2 and air gas flow rates are also set using the mass-flow controller electronics. When the furnace temperature reaches about 450ºC, data recording is initiated in order to document details of the heatup process, including open-cell potential.

Co-electrolysis details were examined by performing stepwise DC potential sweeps, allowing steady-state conditions to be established before recording data at each operating point. Due to the low gas flow rates associated with single-cell testing, about 10 minutes were required at each operating voltage for steady-state conditions to be established at the outlet dewpoint, outlet CO_2, and GC measurement stations. The outlet on-line CO_2 sensor was used primarily to indicate when steady-state conditions were achieved at the outlet. Since these large time intervals were required for steady-state, relatively large voltage increments of typically 100 mV were used in performing the sweeps. Even so, a complete steady-state sweep required about 4 – 5 hours to complete.

IV. DATA REDUCTION

Inlet and outlet gas stream dewpoint temperatures were directly measured in this work. For the co-electrolysis system, the outlet dewpoint value is dependent on the inlet value, the current density, and the shift reaction equilibrium. At open-cell conditions the outlet dewpoint value is higher than the inlet value due to the shift reaction. Measured dewpoints permit direct determination of inlet and outlet steam mole fractions, for comparison against equilibrium predictions. From the measured dewpoint temperatures, water vapor pressures may be calculated from an appropriate correlation (e.g., Antoine's correlation). The inlet and outlet mole fractions of steam can then be obtained from:

$$y_{H2O,i} = \frac{P_{H2O,i}}{P}; \qquad y_{H2O,o} = \frac{P_{H2O,o}}{P} \tag{2}$$

where P is the total pressure at the measurement station, which is directly measured in this study at both dewpoint stations.

It should be noted that since the mole fraction of steam in the inlet gas flow is determined strictly by the dewpoint temperature, the total inlet volumetric flow rate of steam is therefore directly proportional to the sum of the volumetric flow rates of nitrogen, hydrogen and CO_2:

$$Q_{s,H_2O,i} = \frac{\left(Q_{s,N_2,i} + Q_{s,H_2,i} + Q_{s,CO_2}\right) y_{H_2O,i}}{1 - y_{H_2O,i}} \tag{3}$$

The inlet mole fractions of the other components can then be evaluated as the ratio of the molar or volumetric flow rate of each component to the total molar or volumetric flow rate. For example, for carbon dioxide:

$$y_{CO_2,i} = \frac{Q_{s,CO_2}}{\sum_j Q_{s,j}}; \quad \dot{N}_{CO_2} = Q_{s,CO_2} \frac{P_{std}}{R_u T_{std}}; \tag{4}$$

For coelectrolysis, the magnitude of the total steam plus CO_2 flow rates is important in determining whether or not oxygen starvation is likely to occur during electrolysis operation.

An important performance parameter that quantifies the losses associated with the operation of solid-oxide electrolysis cells is the area-specific resistance (ASR). This quantity is defined as:

$$ASR = \frac{V_{op} - V_{ref}}{i} \quad \text{where} \quad i = \frac{I}{A_{cell}} \tag{5}$$

where V_{op} is the applied operating potential, V_{ref} is the reference or open-cell potential and i is the current density (A/cm^2). In calculating area-specific resistance, we have used the reference voltage measured using the reference electrode on the button cell at each operating condition. Although it always represents an open-cell potential, this reference voltage varies slightly from the zero-current value as the current through the active cell is varied. This variation is due to the change in local gas composition at the electrode surfaces during cell operation.

V. CHEMICAL EQUILIBRIUM MODEL

The open-cell potential for the mixed coelectrolysis system can be calculated as a function of temperature using the Nernst equation for either steam-hydrogen or for CO_2-CO, provided the equilibrium composition of the components is used in the evaluating the equation.

Therefore, prior to applying the Nernst equation, the equilibrium composition must be determined at the operating temperature. Our chemical equilibrium coelectrolysis model (CECM) determines the equilibrium composition of the system as follows.

The overall shift reaction that occurs during heatup from the cold unmixed inlet conditions to the hot pre-electrolyzer state can be represented as:

$$y_{0,CO}\,CO + y_{0,CO2}\,CO_2 + y_{0,H2}\,H_2 + y_{0,H2O}\,H_2O \rightarrow y_{1,CO}\,CO + y_{1,CO2}\,CO_2 + y_{1,H2}\,H_2 + y_{1,H2O}\,H_2O \quad (6)$$

where the y_0 values represent the cold inlet mole fractions of CO, CO_2, H_2, and H_2O, respectively, that are known from the inlet gas flow rate and dewpoint measurements. The unknown hot equilibrium mole fractions of the four species at the electrolyzer temperature, prior to electrolysis, are represented by the y_1 values. The three chemical balance equations for carbon, hydrogen, and oxygen corresponding to Eqn. (6) are:

$$y_{0,CO} + y_{0,CO2} = y_{1,CO} + y_{1,CO2} \quad (7)$$

$$2y_{0,H2} + 2y_{0,H2O} = 2y_{1,H2} + 2y_{1,H2O} \quad (8)$$

$$y_{0,CO} + 2y_{0,CO2} + y_{0,H2O} = y_{1,CO} + 2y_{1,CO2} + y_{1,H2O} \quad (9)$$

The final equation invokes the equilibrium constant for the shift reaction:

$$K_{eq}(T) = \frac{y_{1,CO2}\,y_{1,H2}}{y_{1,CO}\,y_{1,H2O}} \quad (10)$$

completing a system of four equations and four unknowns. Simultaneous solution of this system of equations yields the hot inlet composition.

Once the hot inlet equilibrium composition is determined, the Nernst potential can be calculated from:

$$V_N = \frac{-\Delta G_{f,H_2O}(T)}{2F} - \frac{R_u T}{2F}\ln\left[\left(\frac{y_{1,H2O}}{y_{1,H_2}\,y_{O2}^{1/2}}\right)\left(\frac{P}{P_{std}}\right)^{-1/2}\right] = \frac{-\Delta G_{f,CO_2}(T)}{2F} - \frac{R_u T}{2F}\ln\left[\left(\frac{y_{1,CO2}}{y_{1,CO}\,y_{O2}^{1/2}}\right)\left(\frac{P}{P_{std}}\right)^{-1/2}\right] \quad (11)$$

where y_{O2} is the mole fraction of oxygen on the air side of the cells ($y_{O2} \sim 0.21$). Note that the Nernst equation for either steam-hydrogen or CO2-CO yields the same result for the equilibrium system.

The electrolyzer outlet composition can be determined similarly, after accounting for electrochemical reduction of the system. The chemical balance equation for oxygen must be modified to account for oxygen removal from the CO_2/steam mixture. Accordingly, the oxygen balance equation becomes:

$$y_{1,CO} + 2y_{1,CO2} + y_{1,H2O} = y_{2,CO} + 2y_{2,CO2} + y_{2,H2O} + \Delta n_O \quad (12)$$

where Δn_O is the relative molar rate of monatomic oxygen removal from the CO_2/steam mixture given by:

$$\Delta n_O = \frac{I_e}{2F\dot{N}_{Tot}} \quad (13)$$

In this equation, I_e is the total ionic current, given by the product of the stack electrical current and the number of cells (only one in this case), $\dot{N}_{Tot}$ is the total molar flow rate on the CO_2/steam side, including any inert gas flows, and F is the Faraday number. Finally, using the modified oxygen balance equation, the post-electrolyzer equilibrium composition (state 2) can be determined as a function of temperature from simultaneous solution of three chemical balance equations and the equilibrium constant equation.

This calculated final equilibrium composition can be compared to measurements obtained with the downstream dewpoint sensor for steam and with the gas chromatograph for the other gases. However, since these downstream gas composition measurements are obtained at near-room temperatures, these measured compositions are not necessarily expected to agree with predicted outlet compositions evaluated at the furnace temperature. During cool-down from the furnace temperature to room temperature, the gas composition can change, in accordance with the temperature dependence of the shift-reaction equilibrium constant. However, predictions evaluated at some lower "effective" equilibrium temperature, below which the reaction becomes kinetically frozen, can be used for comparison to the measurements.

VI. EXPERIMENTAL RESULTS

Open-cell potentials are monitored continuously during heatup as a system diagnostic. A significant departure of measured open-cell potentials from predicted values can indicate a problem such as a cracked cell or a short circuit. A plot of open-cell potentials measured during heatup with both the active cell (V_{op}) and the reference cell (V_{ref}) is presented in Fig. 3. The gas flow

Table 1. Inlet conditions for DC potential sweeps.

	Sweep 1	Sweep 2	Sweep 3
Q_{N2} (sccm)	35	50	40
Q_{H2} (sccm)	4	3	8
Q_{CO2} (sccm)	8	6	8
$T_{dp,\,i}$ (°C)	55.1	44.6	30.1
Q_{H2O} (sccm)	10.67	7.27	2.93
T_f (°C)	800	800	800

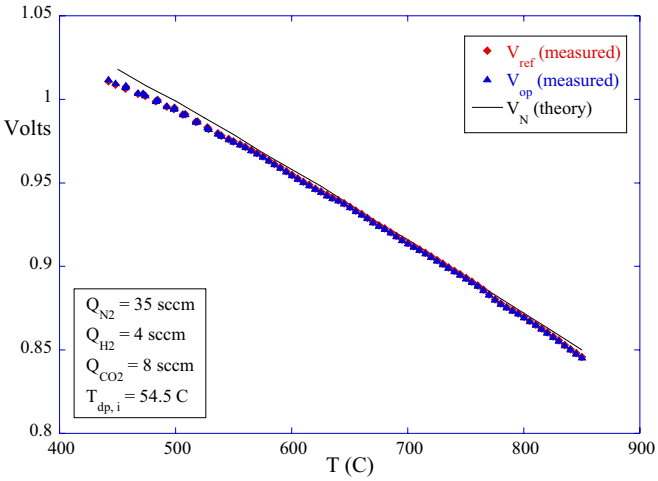

Figure 3. Open-cell potential during heatup, measured and. predicted.

rates and inlet dewpoint values used during the heatup are indicated in the figure. Predicted Nernst potentials based on temperature-dependent equilibrium compositions, and Eqn. (11) are also shown. Above 500°C, agreement between the measured potentials and theoretical values is generally within a few millivolts.

Coelectrolysis performance was characterized through a series of stepwise DC potential sweeps. Results of three sweeps are presented in Figs. 4-6. The furnace temperature for all three sweeps was 800°C. Inlet gas flow rates and inlet dewpoint values for each of these three sweeps are provided in Table 1. The corresponding inlet volume flow rate of steam is also provided in the table. Sweep 1 had the highest steam flow rate; sweep 3 had the lowest. Note that the flow rates used for these test were quite small. Low flow rates were required in order to achieve reasonable steam and CO_2 utilization values with low values of total cell current. The single cell, with an active area of 2.5 cm^2, could only support a maximum total current of about 0.75 A.

Operating voltage, reference voltage, and cell area-specific resistance (ASR, Ohm·cm^2) are plotted in Fig. 4 as a function of current density. In these figures, negative values of current density represent the fuel-cell mode of operation; positive values represent the electrolysis mode. ASR values are based on the reference voltage, per Eqn. (4). Theoretical open-cell voltage (OCV) values corresponding to the equilibrium composition and furnace temperature, calculated using Eqn. (11) are also shown in each figure at zero current density.

Polarization and ASR curves for sweep 1, shown in Fig. 4(a), indicate a relatively high value of ASR in the fuel cell mode at the lowest current density value (-0.068 A/cm^2). This is due to the low inlet hydrogen flow rate used in this sweep. The cell is hydrogen-starved at this operating point, yielding a large concentration overpotential. Otherwise, at higher current densities,

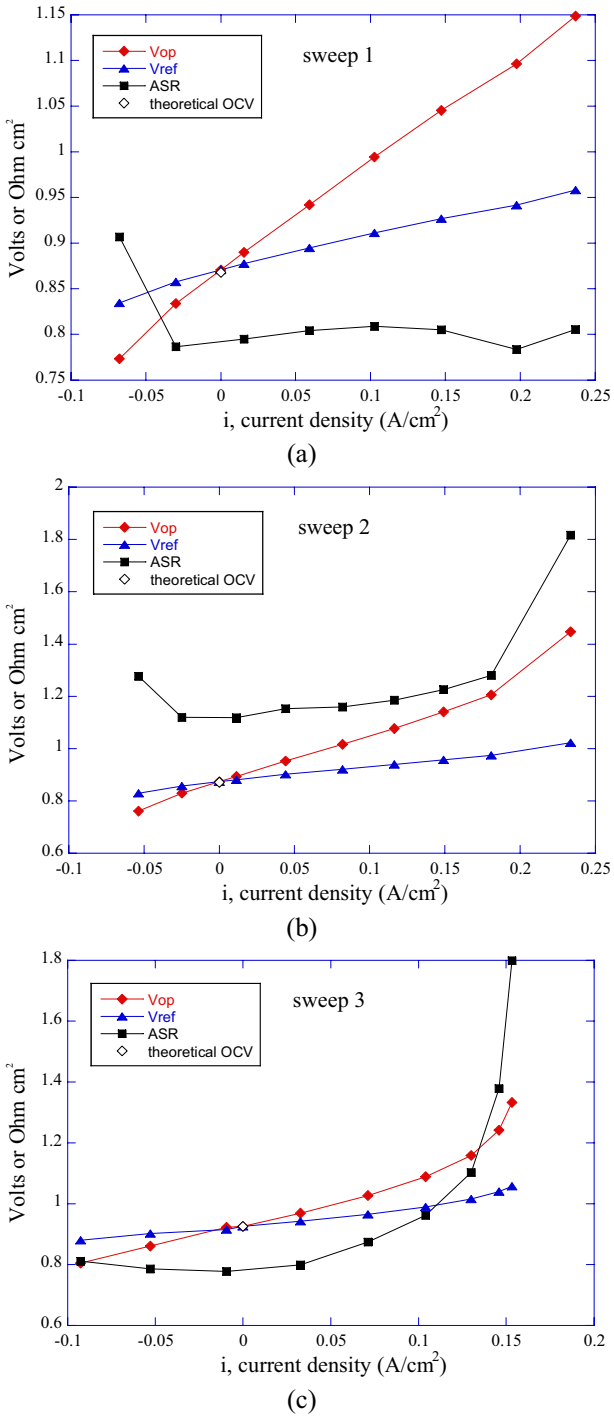

Figure 4. Polarization curves and area-specific resistances for sweeps 1 – 3.

ASR values for sweep 1 are relatively constant, with an average value of 0.80 Ohm·cm^2. The variation in reference voltage shown in these figures is due to the change in local gas composition at the electrode surfaces during cell operation. Since the ASR values plotted in these figures are based on this reference voltage, they represent true ASR values for each operating point.

Polarization and ASR curves for sweep 2, shown in Fig. 4(b), indicate relatively high values of ASR at both current density extremes. High ASR values were observed in the fuel cell mode at a current density of -0.054 A/cm^2 and in the electrolysis mode at 0.233 A/cm^2. At the lowest current density, the high ASR value is related to hydrogen starvation in the fuel cell mode. At the highest current density, the high ASR value is related to oxygen starvation (from CO_2 and steam) in the electrolysis mode. Otherwise, at intermediate values of current density, ASR values for this sweep averaged 1.19 Ohm·cm^2.

Sweep 3 had the highest hydrogen flow rate and the lowest inlet dewpoint value of the three sweeps. Polarization and ASR curves for sweep 3, shown in Fig. 4(c) reflect the low steam content, showing a significant elevation in ASR at the highest current density values. Otherwise, at lower current densities, the average ASR value was 0.79 Ohm·cm^2.

It should be noted that, for similar operating conditions, there was no significant difference between the ASR values measured for pure steam electrolysis and those for coelectrolysis.

The effect of electrolysis on gas composition is shown in Figs. 5 (a – c). These figures plot the mole percent of H_2, CO, and CO_2 as a function of cell current, on a dry basis, for the same three sweeps plotted in Fig. 4. The data symbols represent measurements obtained from the gas chromatograph. The lines represent predictions based on our chemical equilibrium coelectrolysis model (CECM). Two lines are shown for each case. The dashed lines represent CECM predictions based on an effective equilibrium temperature of 700°C. The dotted lines represent CECM predictions based on an effective equilibrium temperature of 650°C.

During coelectrolysis, the mole fractions of CO_2 and steam (not shown in Fig. 5) decrease with current, while the mole fractions of H_2 and CO increase. For the conditions chosen for these tests, the ratio of H_2 to CO is close to the desired 2-to-1 value for syngas production. Measured compositions of CO_2 and CO agree best with predictions based on an effective equilibrium temperature of 700°C. Measured compositions of H_2 agree best with predictions based on an effective equilibrium temperature of 650°C.

The effect of electrolysis on outlet steam content is shown in Figs. 6 (a – c). These figures plot the outlet dewpoint temperature of the process gas mixture as a function of cell current for the same three sweeps presented in Figs. 4 and 5. Outlet dewpoint temperature measurements are obtained from the downstream dewpoint sensor located upstream of the condenser unit and the GC. The inlet dewpoint values for each sweep are listed in Table 1. Note that the zero-current outlet dewpoint values are higher than the inlet dewpoint values, due to the shift reaction. The data symbols in Fig. 6

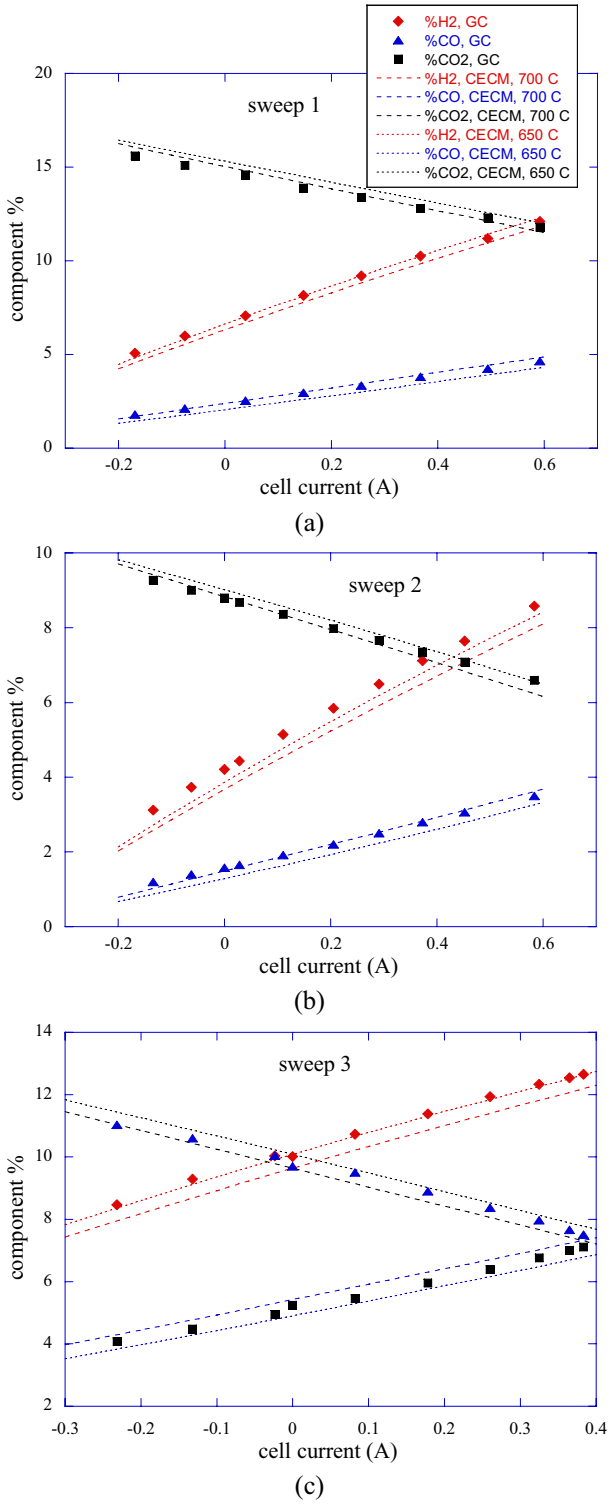

Figure 5. Measured outlet gas compositions, with comparisons to predictions from the chemical equilibrium coelectrolysis model, sweeps 1 – 3.

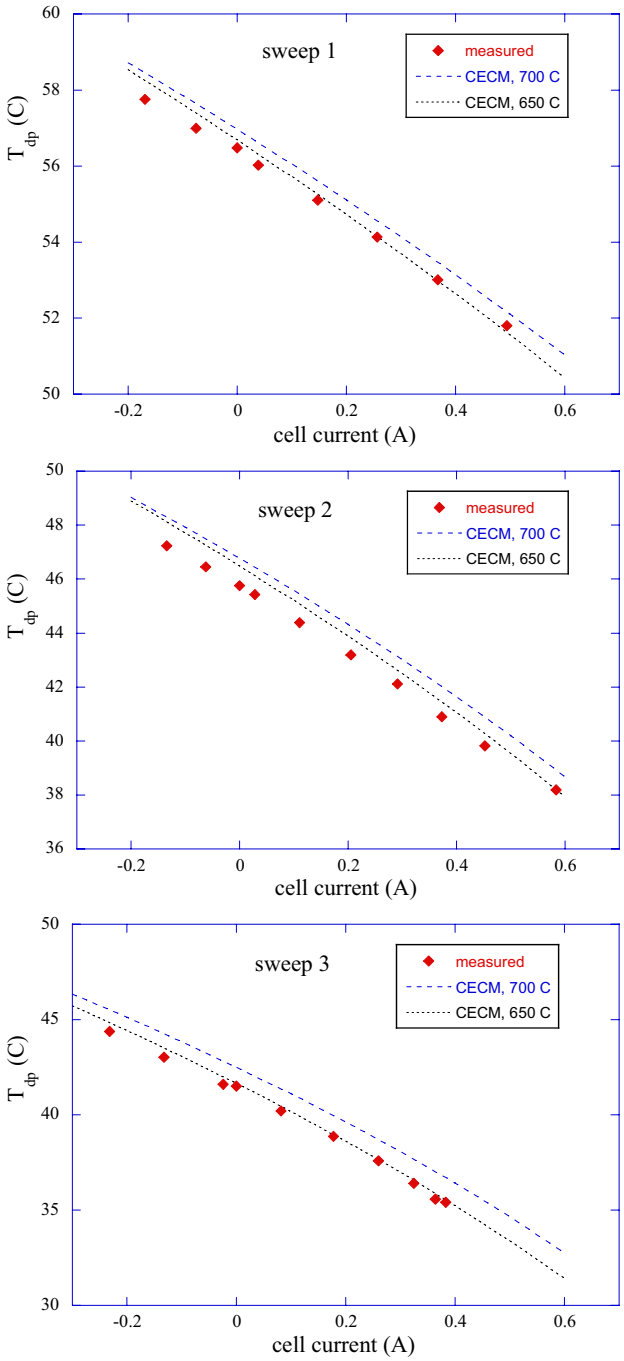

Figure 6. Measured outlet dewpoint values, with comparisons to predictions from the chemical equilibrium coelectrolysis model, sweeps 1 – 3.

represent measurements and the lines represent predictions based on the CECM. Again, the dashed lines represent CECM predictions based on an effective equilibrium temperature of 700°C. The dotted lines represent CECM predictions based on an effective equilibrium temperature of 650°C.

During coelectrolysis, the outlet dewpoint value decreases with cell current. Measured dewpoint values agreed best with CECM predictions based on an effective equilibrium temperature of 650°C. Note that the outlet dewpoint temperature for sweep 3 is quite low at the highest current densities, consistent with the high ASR value observed at this operating condition.

FUTURE WORK

Co-electrolysis experiments have been scaled up and multiple-cell stack testing has been performed. Demonstration of methane formation from the produced syngas is planned for the near future. Detailed system modeling of large-scale coelectrolysis systems will also be performed.

CONCLUSIONS

Based on the results obtained to date, coelectrolysis of steam and carbon dioxide for direct production of syngas appears to be a promising technology that could provide a possible path to reduced greenhouse gas emissions and increased energy independence, without the infrastructure shift that would be required for a hydrogen-based transportation system. Single-cell experimental results indicate good agreement between measured and predicted outlet gas compositions as a function of cell current. Predictions were based on a chemical equilibrium coelectrolysis model.

NOMENCLATURE

A_{cell}	cell active area, cm^2
ASR	area-specific resistance, Ohm·cm^2
F	Faraday number, J/V·mol
ΔG_f	Gibbs energy of formation, J/mol
i	current density, A/cm^2
I	cell current, A
$\dot{N}$	molar flow rate, mol/s
P	pressure, kPa
P_A	partial pressure of component A at inlet, kPa
$Q_{s,A}$	standard volume flow rate of component A
R_u	universal gas constant, J/mol·K
T	temperature, K
V_{op}	cell operating voltage, V
V_{ref}	cell reference voltage, V
y_A	mole fraction of component A

Subscripts

e	electrolysis
0	cold inlet state
1	hot inlet state, pre-electrolysis
2	hot outlet state, post-electrolysis
i	inlet
o	outlet
std	standard state

ACKNOWLEDGMENTS

This work was sponsored by the Idaho National Laboratory, Laboratory Directed Research and Development (LDRD) program and the U.S. Department of Energy, Office of Nuclear Energy, Nuclear Hydrogen Initiative Program.

REFERENCES

1. Forsberg, C. W., "The Hydrogen Economy is Coming. The Question is Where?" *Chemical Engineering Progress*, December, 2005, pp. 20-22.
2. O'Brien, J. E., Stoots, C. M., Herring, J. S., and Hartvigsen, J. J., "Performance of Planar High-Temperature Electrolysis Stacks for Hydrogen Production from Nuclear Energy," *Nuclear Technology*, Vol. 158, pp. 118 - 131, May, 2007.
3. Hawkes, G. L., O'Brien, J. E., Stoots, C. M., Herring, J. S., "CFD Model of a Planar Solid Oxide Electrolysis Cell from Hydrogen Production from Nuclear Energy," *Nuclear Technology*, Vol. 158, pp. 132 - 144, May, 2007.
4. Herring, J. S., O'Brien, J. E., Stoots, C. M., and Hawkes, G. L., "Progress in High-Temperature Electrolysis for Hydrogen Production using Planar SOFC Technology," *International Journal of Hydrogen Energy*, Vol. 32, Issue 4, pp. 440-450, March 2007.